# Long-term economic analysis and optimization of an HT-PEM fuel cell based micro combined heat and power plant

Alireza Haghighat Mamaghani, Behzad Najafi, Andrea Casalegno, Fabio Rinaldi *

*Dipartimento di Energia, Politecnico di Milano, Via Lambruschini 4, 20156, Milano, Italy*

Multi-objective optimization method using genetic algorithm is employed in order to optimize design and operating parameters of a high temperature proton exchange membrane (HT-PEM) fuel cell based combined heat and power system. Net electrical efficiency of the plant, indicating the system's perfor-mance (to be maximized) and the total capital cost (to be minimized) are considered as optimization objectives. Current density (indicating the stack size), steam to carbon ratio, burner outlet temperature and auxiliary to process fuel ratio have been chosen as design parameters. Two different multi-objective optimization approaches have been utilized: steady state (without degradation) and long-term optimization while considering the degradation in fuel cell stack and the fuel processor. The results of the optimization procedures are Pareto frontiers which are a set of optimal points each of which is a trade-off between the considered objective functions. The performance indexes and operating condi-tions of three points with the maximum cumulative net electrical efficiency, minimum capital cost, and the same fuel cell area as that of the initial design are compared. It can be observed that while attempt-ing to maximize the electrical efficiency, the cumulative net electrical efficiency of 29.96% can be achieved although it results in a total capital cost of 115711 €. On the other hand, the capital cost can be reduced down to 39,929 € which significantly diminishes cumulative net electrical efficiency. Finally, by locat-ing the point on the Pareto frontier in which the fuel cell area is the same as that of the initial design, a cumulative net electrical efficiency of 27.07% was achieved which is 1% higher than the value obtained using the operating conditions of the initial design.

***Keywords:*** CHP, PEM fuel cell, Economic analysis, Multi objective, optimization Genetic, algorithm Degradation

HIGHLIGHTS

- Multi-objective optimization is utilized to optimize an HT-PEM fuel cell based CHP plant.
- Net electrical efficiency and total capital cost are considered as optimization objectives.
- A set of optimal points each of which is a trade-off between the objectives is obtained.
- The effect of degradation on the performance of the system is taken into account.

## 1. Introduction

Owing to climate change due to greenhouse-gas (GHG) emissions, inevitable depression of fossil fuels sources and increasingly stringent environmental rules, searching for novel power production technologies based on more efficient and environment-friendly operation can be crucial in near future [1,2]. In the mentioned context, the applications of fuel cells are widespread and encompass large scale stationary power generation in the range of MW to distributed combined heat and power (CHP) and portable power. Moreover, fuel cells benefit from many technological advances including: high conversion efficiency, low emission of pollutants, quiet operation, and the ability to offer electricity and heat simultaneously [3].

Micro-combined heat and power systems (micro-CHP) powered by fuel cells can be used to abate $CO_2$ emissions and supply the domestic energy demand which accounts for a large portion of the total energy consumption and is generally provided by grid electricity and gas fired boilers [4]. On the other hand, in order to follow the concept of distributed generation (DG), stand-alone units based

*Article history:*
Received 8 August 2015
Accepted 5 February 2016
Available online 15 February 2016

* Corresponding author. Tel.: +39 02 2399 2342; fax: +390223993913.
*E-mail addresses:* fabio.rinaldi@polimi.it (F. Rinaldi); alireza.haghighat@polimi.it (A. Haghighat Mamaghani); behzad.najafi@polimi.it (B. Najafi); andrea.casalegno@polimi.it (A. Casalegno).


Published Journal Article available at http://dx.doi.org/10.1016/j.applthermaleng.2016.02.021

on CHP technology can be employed for electrification in remote areas with limited access to the electricity grid. Micro-CHP units can work in parallel with the traditional systems and cover the base demand while grid connection and gas boiler answer the remaining. CHP systems can achieve efficiencies up to 85–90% (combined electrical and thermal efficiency), which is much higher in comparison with the efficiency of the conventional systems generating electricity and heat separately [5].

PEM is the most developed fuel cell technology which is employed in 90% of fuel cell CHP. Thanks to the extensive research conducted in the last decade, today not only have higher efficiency and durability is obtained employing this technology but also its corresponding cost has fallen considerably [6,7]. The low temperature PEM (LT-PEM) fuel cell is the most well-known type of PEM fuel cells which operates at low temperatures (around 80 °C) using a Nafion-based membrane and precious metals loaded electrodes. Several research works have been focused on the application of LT-PEM fuel cells for cogeneration and trigeneration purposes. Ferguson and Ugursal [8] developed a steady state model of a PEM cogeneration fuel cell system to estimating system fuel use, electrical and thermal production, and fuel cell systems sizing. In another study, Radulescu et al. [9] conducted a theoretical and experimental study on different CHP plants based on LT-PEM fuel cell. Modeling and optimization of a micro-cogenerator based on PEM fuel cell was performed by Hubert et al. [10] while considering decrease in natural gas consumption, increase in heat recovery and improve in the water balance as the objectives. El-Sharkh et al. [11] developed a mathematical model in order to locate optimal power output from a PEM fuel cell based power plant.

Nonetheless, LT-PEM fuel cell technology still suffers from some shortcomings which drive researchers to search for solutions. In this regard, one of the most effective options is the operation of the PEM fuel cell at higher temperatures (around 160 °C), the so called HT-PEM fuel cell, which directly affects the stack design and balance of plant (BOP) components that are used for CHP plant. A number of advantages can be attributed to operation at elevated temperature including: simpler water management, lower pressure drop along the channel, cheaper fuel processor given HT-PEMFC stack higher CO tolerance, and simplification of the heat recovery system [12]. A few articles have been fully focused on studying the viability of implementation HT-PEM fuel cells in cogeneration systems. In this context, Arsalis et al. [13] modeled a micro CHP system based on HT-PEM fuel cell stack to cater electricity and thermal demand of a Danish single family household. In this study, a sensitivity analysis has been performed on steam-to-carbon ratio, fuel cell operating temperature, combustor temperature, and hydrogen stoichiometry to investigate their influence on the overall performance of the system. Jannelli et al. [14] compared the performance of three PEM fuel cell based cogeneration plants operating at different temperature levels (67 °C, 160 °C, and 180 °C), and the obtained results suggested that the system based on the HT-PEM fuel cell can achieve electrical efficiencies as high as 40%. In another research study, Zuliani et al. [12] simulated a micro cogeneration system based on a 1 kWel HT-PEM fuel cell using Aspen Plus software and stated that the system can reach the same electrical efficiency as LT-PEM based plant while allowing a simpler balance of plant.

Degradation is one of the main issues concerning the employment of fuel cells in long term which leads to severe voltage drop within the cell and eventually power output plummet. In this regard, degradation's effect on the performance of the fuel cell based CHP plant should be incorporated in the technical and economic evaluations of the system throughout its lifetime [15]. According to a long-term experimental analysis of an HT-PEM based micro-CHP performed by Mocoteguy et al. [16], in the first 500 hours of operation there is no significant drop in stack power output while starting from the 658 hours of cumulated operation the electrical efficiency decreased from 30.6% to 28.3%. In another study conducted by the authors [15], two operational strategies were proposed in order to alleviate the adverse influence of degradation on the long term performance of a fuel cell CHP system.

Economic analysis is an inseparable part of a comprehensive assessment for an energy system which provides the decision maker a clearer understanding of the commercialization capability of a novel system [17–19]. Guizzi et al. [20] investigated the economic and energetic performance of a cogeneration system based on a PEM fuel cell with net electrical and thermal efficiency of 41.93% and 64.16%, respectively, at rated conditions. Hawkes et al. [21] have proposed a model to identify the minimum costs required to meet a given energy demand using a solid oxide fuel cell based CHP. The optimal installed stack capacity under several decision variables such as the stack maximum electrical output capacity and natural gas consumption by the supplementary boiler was then specified. Bianchi et al. [22] proposed a technique for selecting and sizing CHP technologies as well as thermal storage systems based on economic objectives while considering environmental and operational parameters.

In spite of the vast and instructive research in the area of PEM fuel cell based residential CHP systems, there has been a lack of a detailed research in which, considering the long term performance of the unit, the economic aspect of the system is optimized. Motivated by the aforementioned research gap, this paper introduces an approach for the simultaneous optimization of system performance and plant cost while taking into account the degradation within the core components of the system throughout its lifetime. To do so, in the first step, detailed mathematical models of the components of the plant have been developed in the MATLAB environment, which are validated with experimental results. Two multi-objective optimization approaches have been used: steady state (without degradation) and long-term optimization with consideration of degradation during operation. Exploiting the developed models along with the degradation patterns of the fuel cell and stream methane reformer, multi-objective optimization has been performed on the system considering the plant cost and long-term electrical efficiency as competing objectives which should be minimized and maximized, respectively. Next, the performance indexes of three optimal points including the ones resulting to the highest possible cumulative electrical efficiency, the minimum possible capital cost, and an optimal point with the same stack area as the one of initial design are compared. Finally, the resulting lifecycle cost of the mentioned optimal points is investigated to have a better evaluation of the plant's economic aspect.

## 2. Plant description

The configuration of the HT-PEM fuel cell based CHP plant is demonstrated in Fig. 1. The operation principle of the system can be explained as follows: Natural gas is divided into two fuel streams; main one is first desulfurized and then introduced into the SMR reactor and the other stream is fed to the burner as the auxiliary fuel. On the other hand, water is pumped into the steam generator, where it is superheated with the hot gases exiting the SMR reactor. Superheated steam and the desulfurized natural gas are then mixed in the ejector and the mixture is fed to the SMR reactor. The required heat for endothermic reactions within the reformer is provided by the burner where anodic outlet stream which contains unreacted hydrogen and methane is burned with air and auxiliary fuel. The desirable temperature at the burner outlet can be achieved by regulating the amount of air blown into the burner. Through the steam reforming reactions, methane and water are converted into a gaseous mixture of $H_2$, CO, $CO_2$ and unreacted $H_2O$ and $CH_4$. Prior to the WGS reactor, a heat exchanger is employed to reduce the temperature of the WGS inlet stream, considering the exothermic nature

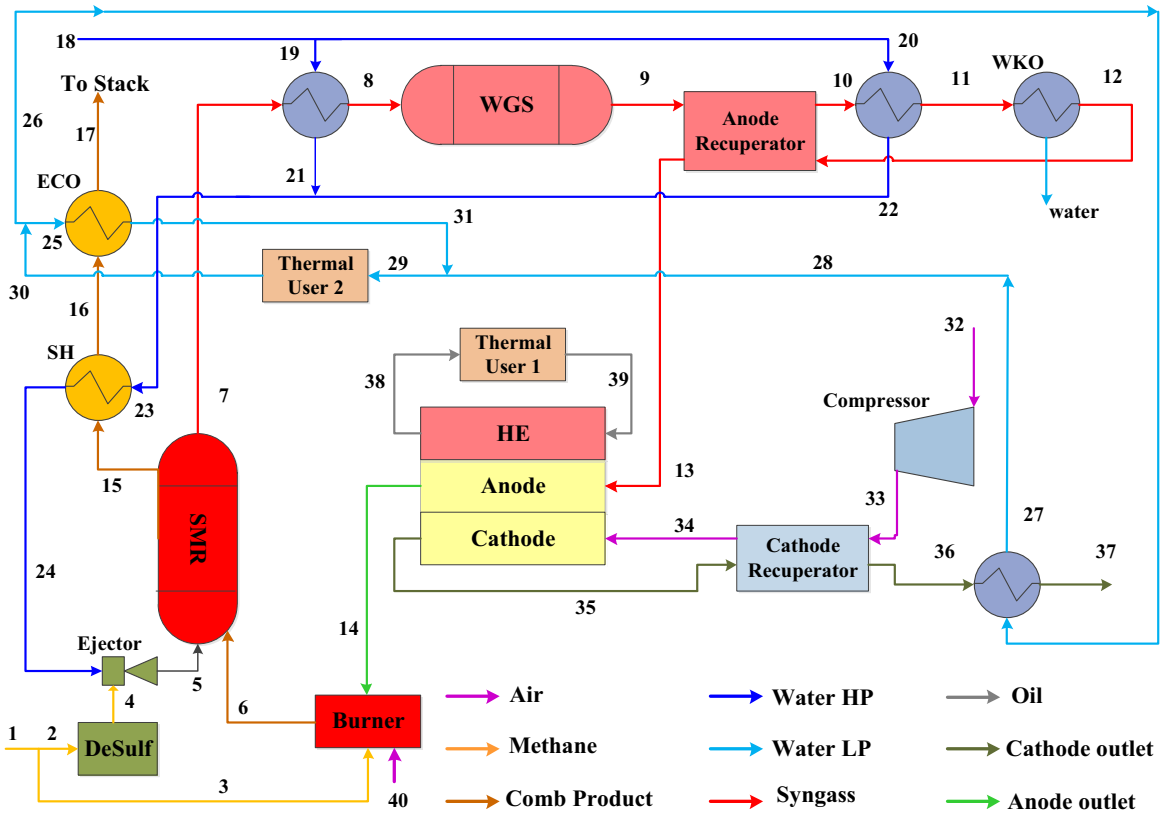


**Fig. 1.** Configuration of the proposed HT-PEMFC based CHP plant.

of WGS reaction, and preheat the water before the superheater. The produced cooled down hydrogen-rich syngas then enters the WGS reactor where carbon monoxide level is reduced into tolerable levels for the HTPEM fuel cell material, and more hydrogen is generated due to the WGS reaction. Before entering the anodic side of the fuel cell, the water content of the syngas (stream 11) is lowered using a water knock-out (WKO). In the fuel cell stack, hydrogen and oxygen participate in the electrochemical reactions and generate electricity, heat, and water. The waste heat produced by the electrochemical reaction is extracted by an oil circulation system and provided to Thermal User 1. The additional heat demand is answered by the low-pressure water circuit which extracts thermal energy from the plant using the economizers and releases it to Thermal User 2. It should be mentioned that the system is considered connected to a grid network to import/export electricity in case there is a mismatch between the production and consumption. Moreover, an external boiler is implemented to cover the surplus heat demand in some periods of the year. A schematic representation of the system interaction with the electricity grid, external boiler and the electricity and heat consumer is illustrated in Fig. 2.

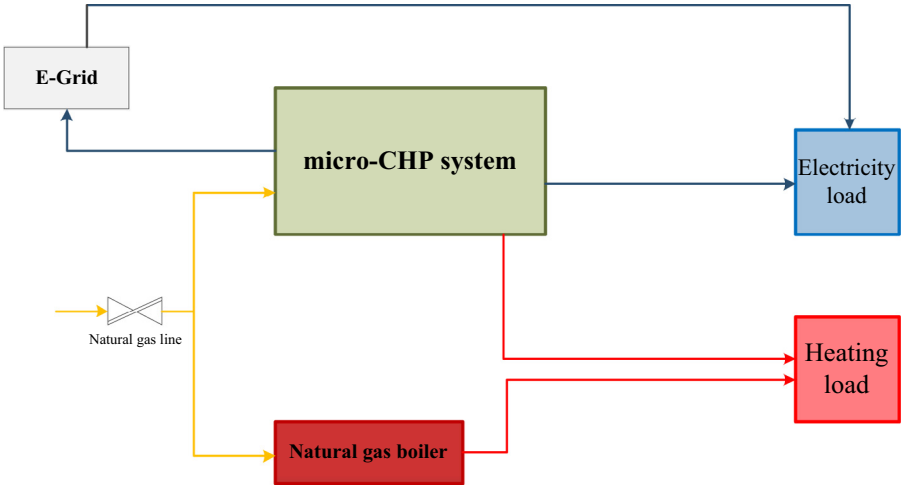


**Fig. 2.** Schematic representation of the proposed system in connection with grid, external thermal source, and consumer.

## 3. Model description

### 3.1. Fuel processor

#### 3.1.1. Steam methane reformer

In the present study, in order to provide the required hydrogen for electrochemical reaction, a steam methane reformer (SMR) has been utilized. A 1D steady state and non-isothermal plug flow reactor has been utilized to model the SMR reactor. In order to model the corresponding reaction kinetics, the model proposed by Xu and Froment [23] has been employed. The experimental data provided by the industrial partner, ICI Caldaie S.p.A, is next employed to validate the developed model. The tube side stream which undergoes the reactions and the shell side combustion gases, providing the required heat for endothermic reactions, are simultaneously simulated. Owing to the confidentiality of the manufacturer's data, the catalyst structure and composition are not reported. The main reactions occurring within the steam reformer are listed below:

$$CH_4 + H_2O \Leftrightarrow CO + 3H_2 \qquad \Delta H_{298K} = +206\,kJ/mol \tag{1}$$

$$CO + H_2O \Leftrightarrow CO_2 + H_2 \qquad \Delta H_{298K} = -41\,kJ/mol \tag{2}$$

$$CH_4 + 2H_2O \Leftrightarrow CO_2 + 4H_2 \qquad \Delta H_{298K} = +165\,kJ/mol \tag{3}$$

Xu and Froment [23] proposed a general model for methane steam reforming in which the water–gas shift reaction and the steam reforming reactions take place in parallel. The kinetic coefficients and the considered assumptions of the model can be found in [23].

#### 3.1.2. Water gas shift reactor

Employing water gas shift reactor leads to both hydrogen yield enhancement and carbon oxide content reduction each of which results in higher electrical efficiency. The kinetic model developed by Keiksi et al. [24] for high temperature WGS has been utilized. It is worth mentioning that the heat exchanger located upstream of to the WGS reactor reduces the temperature of the syngas to a desired level for WGS reaction. The WGS reaction's equilibrium constant can be determined through the following relation [25]:

$$K_p = e^{\left(\frac{4400}{T} - 4.036\right)} \tag{4}$$

The kinetic equation, proposed by Keiksi et al. [24], is as follows:

$$r_{WGS} = k_0 . \exp\left(\frac{-E_a}{RT}\right)(1-\beta) P_{CO}{}^{1.1} P_{H2O}^{0.53} \tag{5}$$

where $E_\alpha = 95000$ kJ/mol is the activation energy, R = 8.314 J/(K.mol), ln ($k_0$) = 26.1 is pre-exponential factor, and β is the reversibility factor calculated by:

$$\beta = \frac{1}{K_P}\frac{P_{CO_2} P_{H_2}}{P_{CO} P_{H_2O}} \tag{6}$$

### 3.2. HT-PEM fuel cell stack

Aside from the MEA, the HT-PEM fuel cell stack also includes a pre-heater and the oil cooling circuit. The reactants, before entering the MEA, go through the pre-heater in which they reach the stack temperature by exchanging heat with the circulating oil. In the MEA, as a result of the electrochemical reaction, hydrogen and oxygen are consumed while water and electricity are produced. The MEA is made up of three main parts including the cathodic and anodic channels, the gas diffusion layer (GDL) and the anodic and cathodic electrodes. The reactants pass through the GDL to reach the catalyst layer where they undergo the electrochemical reaction. The polybenzimidazole (PBI) membrane separates the cathodic and anodic electrodes. The geometrics of the stack are as follows: the length, height, and number of channels are 76.25 cm, 0.2 cm, and 38 respectively, and the cell width is 7.6 cm.

A quasi 2D approach is employed to model the MEA domain. Accordingly, the integration is carried out in two coordinates: along the channel and along the thickness of the MEA. Owing to the electrochemical reaction taking place through the channel, hydrogen and oxygen are gradually consumed while water is consequently generated. Mass conservation is employed in order to find the concentration profiles of the species.

The current density is calculated employing the following equation:

$$V = E_{ID} - \eta_{OHM} - \eta_C - \eta_A \tag{7}$$

$$P_{stack} = V_{cell} I_{stack} N \tag{8}$$

where V is the single cell voltage, $E_{ID}$ is the ideal voltage by Nernst equation, $\eta_{OHM}$ is the ohmic loss, and $\eta_C$ and $\eta_A$ are the cathode and anode activation losses, respectively. $E_{ID}$ (Ideal voltage) is determined as a function of temperature from the Gibbs free energy formation data.

The Ohmic loss determined by summing up the bipolar plates, GDLs, and the electrolyte resistances while assuming that it follows the Ohm's law. The electrolyte conductivity is also presumed to follows the Arrhenius law and it is taken from [26]. The electrolyte's proton conductivity is employed to determine its Ohmic loss:

$$\eta_{ohm} = \frac{i\delta_m}{\sigma_{PBI/H_3PO_4}(T)} \tag{9}$$

where

$$\sigma_{PBI/H_3PO_4}(T) = \frac{\sigma}{T} exp\left(-\frac{E_a}{RT}\right) \tag{10}$$

In order to simulate the mass transport within the GDL, Stefan–Maxwell law [27] is employed. The cathodic electrode's activation losses are assumed to follow the Tafel Law, first order with respect to oxygen concentration [28]:

$$\eta_C \equiv b \cdot \log\left(\frac{i}{i_*}\right) + b \cdot \log\left(\frac{C_{ref}}{C_{O_2,el}}\right) \tag{11}$$

where $i_*$ is the reference exchange current density following an Arrhenius like behavior and $b$, the Tafel slope, is calculated employing using the following relation:

$$b = RT/(\alpha_C F). \tag{12}$$

Carbon monoxide poisoning can have a considerable influence on the cell voltage and subsequently the performance of the fuel cell; accordingly, the corresponding effect has been considered. The carbon monoxide and hydrogen oxidation currents are calculated employing using Butler–Volmer equation [29] :

$$i_{H2} \equiv i_{*,H2} \cdot \vartheta_H \cdot 2\sinh\left(\frac{\eta_A}{b_A}\right) \tag{13}$$

$$i_{CO} \equiv i_{*,CO} \cdot \vartheta_{CO} \cdot 2\sinh\left(\frac{\eta_A}{b_A}\right) \tag{14}$$

$$i = i_{CO} + i_{H_2} \tag{15}$$

in addition, sum of the coverage of all the species is equal to 1; accordingly:

$$\vartheta_{FREE} = 1 - \vartheta_H - \vartheta_{CO} - \vartheta_{H_2PO_4}. \quad (16)$$

Phosphoric acid's coverage ( $\vartheta_{H_2PO_4-}$) is found from the data given by [30]. The Frumkin adsorption for carbon monoxide and the Langmuir adsorption for hydrogen, while assuming the adsorption equilibrium, are utilized to determine the carbon monoxide and the hydrogen coverage ( $\vartheta_{CO}$ and $\vartheta_H$ ). The parameters employed while developing HT-PEM fuel cell stack model can be found in the previous article of the authors [31].

## 4. System optimization

### 4.1. Definition of objective functions

In this study, two different optimization approaches have been introduced based on steady state operation of the plant and the long-term one which takes into account the degradation within the main components. In the first procedure (Optimization procedure I), the net electrical efficiency and the capital cost of the plant are defined as objective functions while considering two different levels of fuel partialization to cover a broader range of generated thermal and electrical power. In the second approach (Optimization procedure II), the cumulative net electrical efficiency and the plant capital cost are considered as the objective functions as the system is investigated for the first 15,000 hours of its operation given the degradation in SMR and fuel cell. It is worth mentioning that the inlet fuel flow rate fed to the plant is changing in the optimization process due to the variation of the auxiliary to process fuel ratio, though the process fuel fed to the SMR is kept constant.

The net electrical efficiency considered in the second optimization procedure is defined as follows:

$$\eta_{net,el} = \frac{\dot{P}_{el,net}}{\dot{m}_{CH_4,in} LHV_{CH_4}} \quad (17)$$

where the net power output ($\dot{P}_{el,net}$) is the power produced by the fuel cell stack after subtracting losses and auxiliaries.

The cumulative net electrical efficiency is similarly defined as:

$$\eta_{cum,net,el} = \frac{\sum_{i=1}^{6} \Delta t_i . P_{net,el,i}}{\sum_{i=1}^{6} \Delta t_i \dot{m}_{CH_4,in,i} LHV_{CH_4}} \quad (18)$$

The 15,000 hours of operation is divided into six time periods considering the degradation trends for SMR and the stack. In each time interval, the mean degradation value of that period has been used for $\dot{P}_{el,net}$ and $\dot{m}_{CH_4,in}$ calculation and in the optimization process and the obtained results are representatives of the entire period.

The presented economic analysis takes into account the total capital cost of the plant which constitutes of the capital cost of each component in the plant. The cost for fuel processor and balance of plant have been calculated based on a cost estimation suggested in Ref. [32] and the values are 335 $/kW and 297 $/kW, respectively. In order to estimate the cost of the fuel cell stack, the values reported by Arsalis [33] and the industrial partner has been used which is 0.24 $/cm$^2$ for the HT-PEM fuel cell. It should be mentioned that in each level of fuel partialization, the size of fuel processing system and BOP are fixed and only the fuel cell stack design varies based on the design parameters.

### 4.2. Design parameters and constraints

Current density (i), steam to carbon ratio (S/C), burner outlet temperature ($T_B$), and fuel auxiliary to process ratio (aux/proc) were selected as the design parameters. A number of constraints and ranges for design parameters have been respected during the optimization procedure in order to certify the technical feasibility of the optimization results. The selected design parameters and their range of variation along with the corresponding constraints are listed in Table 1.

**Table 1**
List of constraints for system optimization and the range of variation of design parameters [15,34].

| Constraint | Reason |
|---|---|
| $3.5 < S/C < 5.5$ | Minimum and maximum values of steam to carbon ratio |
| $1000 < i_{cell} < 4000$ A.m$^{-2}$ | Minimum and maximum values of cell current density |
| $1100 < T_B < 1300$ K | Minimum and maximum values of burner outlet temperature |
| $0.12 <$ Aux/Proc $< 0.22$ | Minimum and maximum values of auxiliary to process fuel ratio |
| $T_8 < 610$ K | Due to exothermic nature of WGS reaction |
| $T_{17} > 340$ K | To avoid formation of carbonic acid ($H_2CO_3$) in exhaust gases |

### 4.3. Optimization method

Multi-objective optimization is an effective approach to deal with many engineering problems which require simultaneous optimization (i.e. minimizing or maximizing) of more than one objective function while complying a number of equalities and inequalities. Expectedly, the obtained result for a multi-objective optimization problem, unlike single-objective optimization problems, is not a unique point since no single solution can satisfy the conflicting objectives at the same time without sacrificing one of the objectives. As a result, in multi-objective optimization the goal is to find a set of solutions which satisfy the objective functions at a satisfactory level without being dominated by other solutions. After obtaining the set of solutions, called the Pareto front, based on the specific application one can decide which design set is the most suitable. In the present study, the genetic algorithm (GA) technique was utilized to optimize the aforementioned objective functions by variation in the design parameters and locating the best solutions. The details of the employed optimization method as well as the mechanism of selecting design parameters in order to reach the final set of solutions can be found in the literature [34,35]. The multi-objective GA implemented in MATLAB optimization toolbox has been employed in the present work for 200 generations, considering population size of 300 individuals, cross over probability of 0.9 and gene mutation probability of 0.01.

### 4.4. Lifecycle cost definition

In order to put together the two competing objectives in a single criterion, the lifecycle cost of the plant during the period of operation has been determined which constitutes the income from electricity and heat sell and operating and investment cost. The plant is considered to be grid-interconnected; so importing the electricity from the grid in peak load and exporting it to the grid in periods with low demand is possible. The operating cost is calculated based on the fuel unit cost and the fuel consumption while the investment cost is the sum of capital costs of all the components at the beginning of the operation as explained in section 4.1. To calculate the lifecycle cost, the following correlation has been employed:

$$LCC = \dot{Z}_{plant} . t + c_f . \dot{m}_f . t - c_{el} . E_{ele,total} - c_{th} . E_{th,total} \quad (19)$$

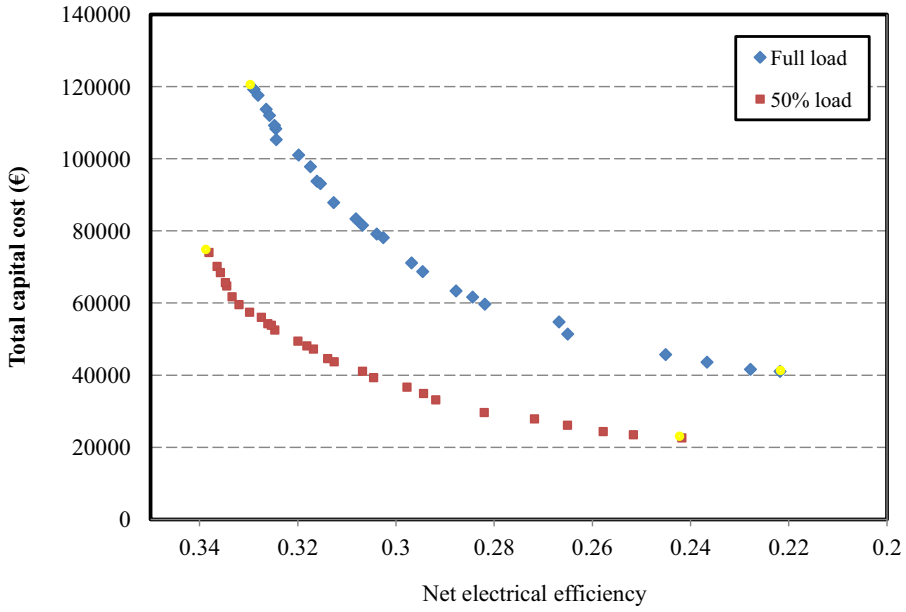


**Fig. 3.** Pareto front obtained from multi-objective optimization procedure I in full and partial load.

$\dot{Z}_{plant}$ is the capital cost per unit of time and is calculated based on the capital recovery factor considering the interest rate of 1.14% in Italy and maintenance factor of 1.08 for six years of operation [35]. The overall capital cost is the sum of the cost of components given in the section 4.1. The unit cost of fuel ($c_f$) is considered 46 $c€/m_n^3$ with reference to Italian market and the selling price of electricity ($c_{ele}$) and heat ($c_{th}$) are 4.72 c€/MJ and 1.47c€/MJ, respectively [20].

It should be mentioned that the income of providing heat by the CHP system is calculated based on a comparison with a natural gas boiler producing the same amount of energy. It is also noteworthy that the income for produced electricity and heat are determined based on the total energy production in 15,000 hours and the cost per unit of energy for electricity and heat.

## 5. Results and discussion

### 5.1. Reformer and HT-PEM stack model validation

The kinetic characteristics and geometric parameters of the water gas shift and steam methane reformer reactors are the same as the ones of an LT-PEM fuel cell based CHP plant (Sidera30), designed and tested by the industrial partner (ICI Caldaie S.p.A.). Therefore, the validation of the fuel processor system model has been performed using the syngas composition at the outlet of the reformer and WGS reactor and the temperature of the syngas leaving the fuel processor reactors and the superheater outlet temperature.

Validation of the HT-PEM fuel cell model has been done by comparing the polarization curves of the fuel cell obtained from the simulation and the experimental data given by Bergmann et al. [30], at different temperatures (130–160 °C) and CO concentrations in the anode inlet stream. The comparison between the polarization curves from the present work and the literature shows a subtle difference which verifies the accuracy of the developed model for investigating the behavior of the HT-PEM fuel cell. Details of the fuel processor and fuel cell model validation were given in the previous work of the authors [15,31].

The data related to degradation within the steam reformer and the fuel cell stack through time have been reported in the previous work of the authors [31,36] and Kim et al. [37]. Given the similar characteristics of the fuel cell employed in the present work and the one studied by Kim et al. [37], the model proposed by Kim et al. [37] has been employed in the present study to predict the degradation within the HT-PEMFC stack.

### 5.2. Steady state operation optimization

As the first analysis, the steady state optimization of the plant at the beginning of operation (time = 0) has been investigated for full load operation and 50% fuel partialization. The central reason for having two levels of fuel partialization is to provide a broader range of operation and design which in turn enables the customer to choose the most suitable system for a specific application based on investment cost and performance indexes. For each solution vector selected by the genetic algorithm, an iterative procedure has been applied with guess values for anodic outlet stream and the superheated steam temperature to find the converged results of the performance of the system and the plant capital cost. Utilizing the developed component models, the composition, mass flow rate and the temperature at each point of the plant are calculated and the determined values of anodic outlet stream's composition and the superheated water temperature are compared with the guess values. The iteration continues until the differences between the guessed and calculated value are less than the assumed tolerance.

Fig. 3 exhibits the Pareto frontier obtained from the multi-objective optimization on the HT-PEM fuel cell based CHP plant using genetic algorithm method. This figure clearly points out the competing relation between the economic objective (plant's capital cost) and the thermodynamic one (net electrical efficiency). As the net electrical efficiency enhances, the total capital cost of the plant rises which sets a constraint on steady growth in electrical efficiency. As it can be seen in the figure, the optimization results offer a wide range of investment cost starting from 20,000 € up to 120,000 €. A major portion of the capital cost is related to the high cost of HT-PEM fuel cell considering the fact that it is a new technology and until mass production and commercialization, HT-PEM fuel cell CHP suffers from substantial economic disadvantage compared to conventional energy production systems. On the other hand, given different combinations of design parameters selected by genetic algorithm, net electrical efficiency varies between 22% and 34%.

**Table 2**
Design parameters and performance indexes of the system for extreme cases at different partialization levels (optimization procedure I).

| Parameter | Full load operation | | 50% fuel partialization | |
|---|---|---|---|---|
| | Extreme in favor of $\eta_{ele}$ | Extreme in favor of capital cost | Extreme in favor of $\eta_{ele}$ | Extreme in favor of capital cost |
| S/C | 4.49 | 4.01 | 4.51 | 4.78 |
| i ($A.m^{-2}$) | 1005 | 4000 | 1037 | 3990 |
| $T_B$ | 1221.3 | 1180.1 | 1225.1 | 1208.2 |
| Aux/Proc | 0.134 | 0.120 | 0.151 | 0.216 |
| $\eta_{ele}$ (%) | 32.89 | 22.18 | 33.81 | 24.17 |
| $\eta_{th}$ (%) | 50.81 | 61.34 | 48.06 | 57.58 |
| $\eta_{sys}$ (%) | 83.70 | 83.52 | 81.87 | 81.57 |
| $P_{ele}$ (kW) | 31.37 | 20.89 | 16.38 | 12.47 |
| $P_{th}$ (kW) | 48.47 | 57.77 | 23.26 | 29.45 |
| Stack cost | 102,328 | 24,142 | 65,451 | 14,030 |
| Fuel processor cost | 8831 | 8831 | 4450 | 4450 |
| BOP cost | 8100 | 8100 | 4150 | 4150 |
| TCC (€) | 119,260 | 41,074 | 740,51 | 22630 |

The extreme cases which can be noticed in Fig. 3 are the highlighted end points on the curves in which thermodynamic objective (net electrical efficiency) is most weighted (upper left corner) and on the other end, economic objective (total capital cost) is most weighted (bottom right corner). The values of design parameters as well as the performance indexes corresponding to these points are given in Table 2. It should be mentioned that partialization of the fuel not only leads to lower capital cost for the plant, but also brings about lower operating cost which is mainly due to the natural gas consumption. Furthermore, as can be noticed in the table, the share of HT-PEM fuel cell's cost in the total capital cost is considerable which stems from the fact that unlike BOP components and fuel processor system (SMR and WGS reactors), HT-PEM fuel cell is still in the research and development stage. As a consequence, until complete commercialization, the capital cost of HT-PEMFC CHP is considerably higher than the conventional energy production units.

By monitoring the variations of design parameters for the optimal points on the Pareto frontier curve, two conclusions can be drawn. First, the ranges of variation of steam to carbon ratio, burner outlet temperature, and fuel auxiliary to process ratio are narrow which suggest that for optimization, one may choose any value in these optimum ranges without sacrificing any of the objective functions. Second, current density is the most influential design parameter which in fact plays the key role in obtaining the trade-off between the two objective functions. On one hand, increasing the current density results in smaller required area for the fuel cell stack which in turn decreases the capital cost, but on the other hand, higher current density means higher voltage losses (based on polarization curve) within the stack which deteriorates the net electrical output and subsequently net electrical efficiency. The distribution of current density for the solutions given by the Pareto front at full load is presented in Fig. 4.

### 5.3. Long-term optimization

The second optimization procedure has been focused on the operation of the system in long-term while bearing in mind the economic aspect of the plant. In this regard, the optimization has been carried out for the first 15,000 hours of operation of the system considering the degradation within the fuel cell and reformer and its effect on the cumulative net electrical efficiency and capital cost of the plant. It should be pointed out that the system is assumed to only be employed during the cold seasons in Italy in which, based on demand, system can provide both electricity and heat and there is no need to discard the generated thermal energy in the plant.

Fig. 5 shows the obtained Pareto frontier curve for the long-term optimization of the HT-PEM fuel cell CHP with cumulative net electrical efficiency and total capital cost as objectives. The conflicting relation between the economic and thermodynamic objectives can be clearly seen in this figure; so, as the efficiency improves, the capital cost increases. Each of the represented points in the Pareto front curve can be recognized as the optimum achievable cumulative net electrical efficiency for that specific capital cost. As a result, based on the decision maker budget or the target electrical efficiency for the 15,000 hours of operation, any point can be selected from the Pareto solutions guaranteeing the best combination of cost and efficiency.

Fig. 6 depicts the variation of design parameters for the given solutions in the long-term Pareto front (Fig. 5). As it can be easily noticed, all the parameters except current density are restricted to a narrow optimum range for all the Pareto solutions while the current density sweeps its whole operating range and is the main origin of the obtained Pareto curve. Increasing the current density on the one hand leads to lower electrical efficiencies due to higher voltage losses (according to the polarization curve) but on the other hand, higher current density causes lower required fuel cell active area which means lower capital cost for stack.

Three optimal points including the one with maximum possible cumulative net electrical efficiency (point A), minimum possible capital cost (point B), and the point with the same employed fuel cell area as that of the initial design (point C) have been selected on the Pareto curve for further investigation (as showed in Fig. 5). The performance indexes of the system at selected optimal points in each time interval are summarized in Table 3. Due to the fact that the fuel fed to the system is kept constant, in each set of operating parameters for 15,000 hours, the trends of electrical and thermal efficiency correspond to the generated electrical power and thermal output variation, respectively. As can be noticed, electrical generation experiences a descending trend throughout the operational life of the system while thermal output augments with time. The observed downward trend in the electrical generation values in the first few thousand hours of operation can be attributed to the severe degradation in the SMR, while at the end of the investigated period degradation of the stack is more considerable. Regarding the behavior of thermal output, as can be seen in Table 3, its growth stems from two different sources. First of all, the waste heat produced in the fuel cell increases with time due to degradation which leads to higher voltage losses within the stack. Second, SMR catalyst degradation hinders the endothermic reforming reaction which causes higher outlet temperature of the combustion gases exiting

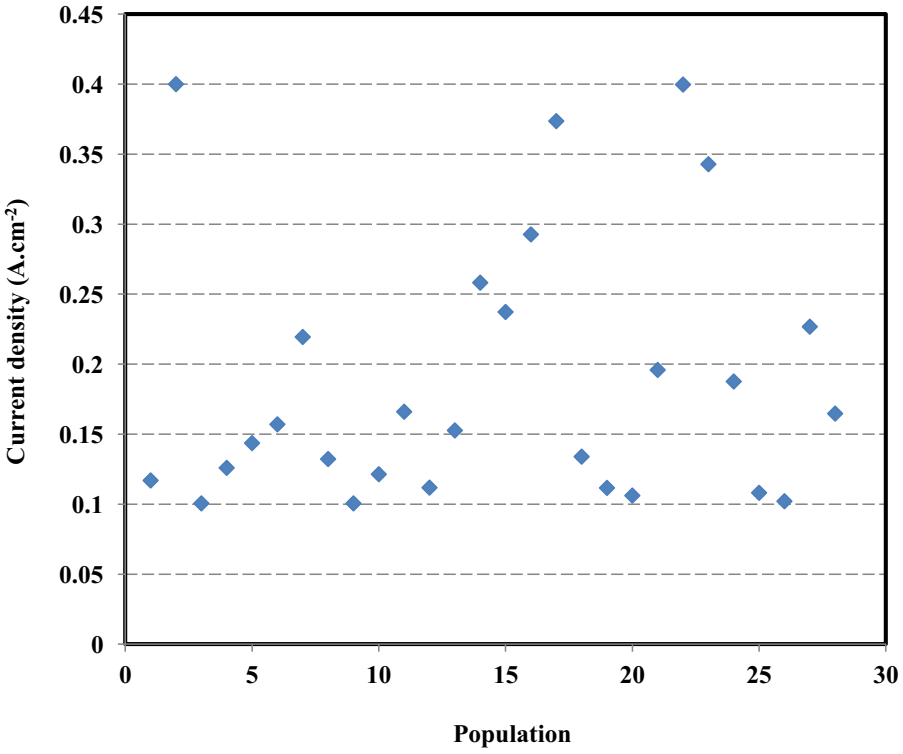


**Fig. 4.** Distribution of current density values for optimization procedure I at full load.

reformer which in turn boosts the economizer thermal gain and the overall thermal output.

The design parameters, overall cumulative performance indexes, and economic criteria corresponding to points A, B and C are brought in Table 4. As can be seen in this table, employing the operating conditions of Point A results in a cumulative net electrical efficiency of 29.96% and a total capital cost of 115,711 €. On the other hand, by utilizing the design conditions of Point B, which leads to the lowest possible capital cost, the cumulative net electrical efficiency is reduced down to 18.36%, and the required capital cost is also decreased to 39,929 €. Finally, in order to compare the performance of the optimized system with the one of the initial design, the performance indexes of the optimal point in which the fuel cell area is the same as that of the initial design are monitored. It was observed that a cumulative net electrical efficiency of 27.07% can be achieved which is almost 1% higher than the corresponding index

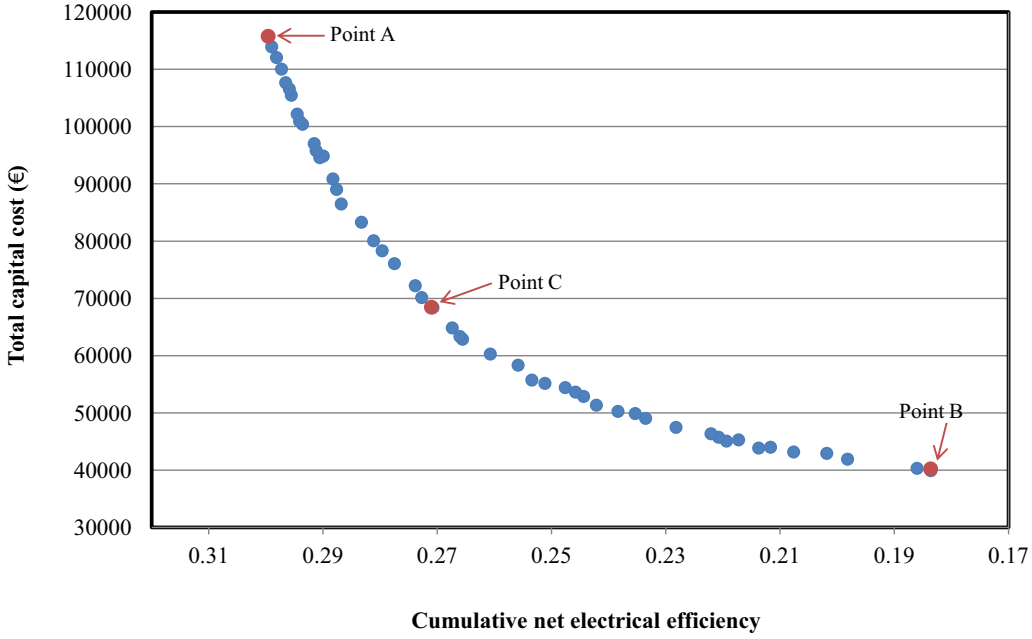


**Fig. 5.** Pareto front obtained from long-term multi-objective optimization procedure II.

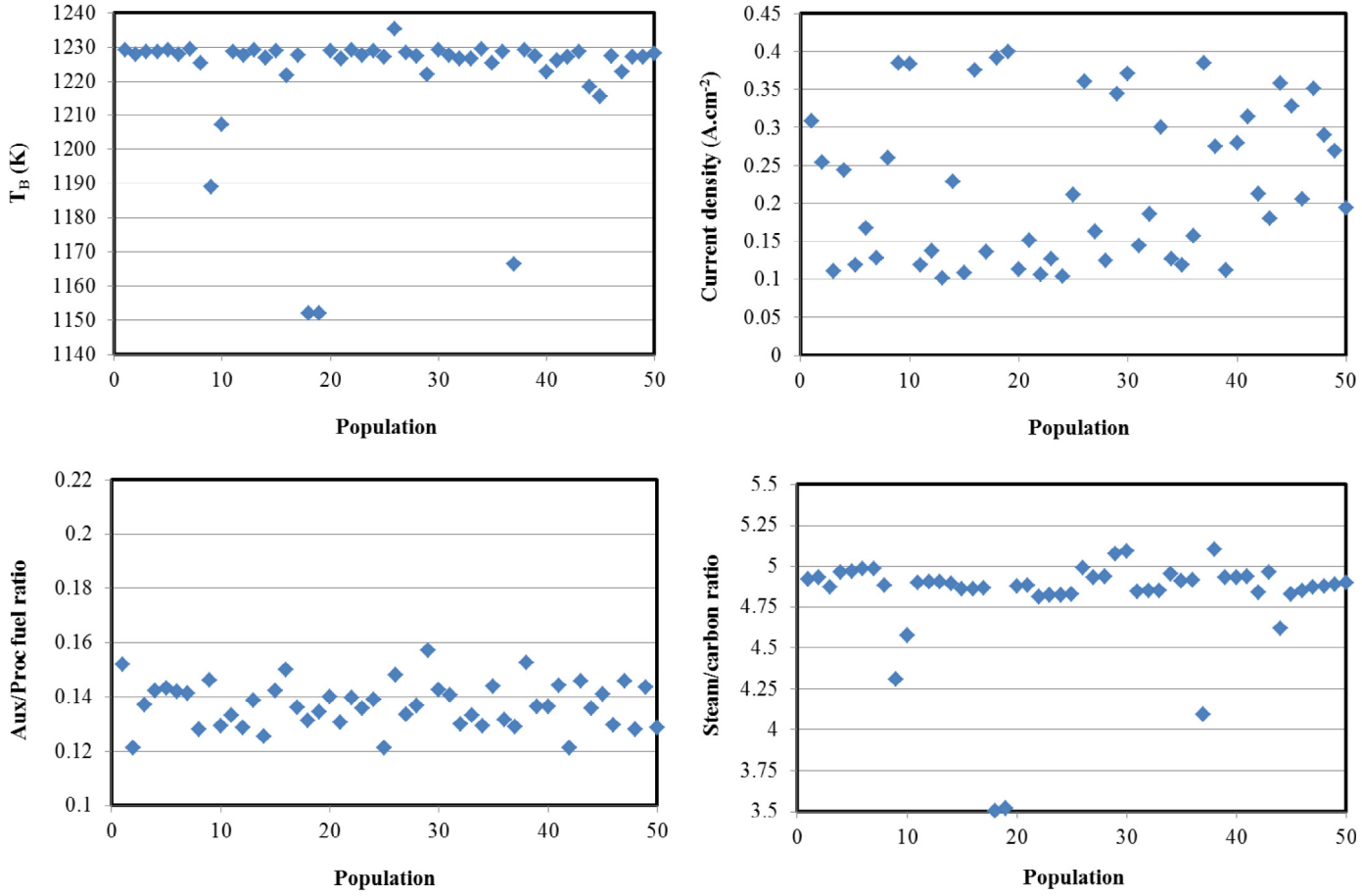


**Fig. 6.** Distribution of design parameters for multi-objective optimization procedure II.

which was obtained using the initial design of the system reported in the previous study of the authors [15].

The values of lifecycle cost of the chosen optimal points are demonstrated in Table 4. It can be observed that, owing to the higher weight of the fuel cell stack's cost, Point B in which the economic cost is minimized also results in the lowest possible lifecycle cost of 16,736 €. It is worth noting that in countries with higher electricity cost and lower natural gas price, the lifecycle cost will be considerably lower than the calculated value for Italy. The economic viability of the proposed HT-PEM CHP plant strongly depends on the capital cost of the fuel cell stack as well as its degradation rate and durability. Consequently, considering the steady downward trend in the production cost of HT-PEM fuel cell and the government's incentives for high efficiency CHP plant, in the next years, cogeneration plants based on HT-PEMFC can have a higher possibility of reaching the commercialization stage.

## 6. Conclusion

A long-term economic and optimization of an HT-PEM micro-CHP system has been performed in the present work. Employing the experimentally validated models of core components of the plant, the BOP model, and the degradation patterns in the MATLAB® environment, the genetic algorithm multi-objective optimization approach has been used considering total capital cost and net electrical efficiency as objective functions. For the optimization, current density, steam to carbon ratio, burner outlet temperature and auxiliary to process fuel ratio have been chosen as design parameters. In the first part of the paper, a steady state optimization has been performed and the resulting Pareto front has been demonstrated. In the second part of the article, a long-term optimization method has been applied while considering the degradation within reformer and stack and its effect on the cumulative net electrical efficiency.

**Table 3**
The values of performance indexes for selected points at different time intervals (optimization procedure II).

| | Parameter | | | | | | | | | | | |
|---|---|---|---|---|---|---|---|---|---|---|---|---|
| | Point A | | | | Point B | | | | Point C | | | |
| Time interval (hour) | $\eta_{ele}$ (%) | $\eta_{th}$ (%) | $P_{ele}$ (kW) | $P_{th}$ (kW) | $\eta_{ele}$ (%) | $\eta_{th}$ (%) | $P_{ele}$ (kW) | $P_{th}$ (kW) | $\eta_{ele}$ (%) | $\eta_{th}$ (%) | $P_{ele}$ (kW) | $P_{th}$ (kW) |
| 0–500 | 32.08 | 48.98 | 30.73 | 46.92 | 20.64 | 64.26 | 19.7 | 61.32 | 29.28 | 51.09 | 27.8 | 48.5 |
| 500–1500 | 31.71 | 50.05 | 30.37 | 47.94 | 20 | 65.04 | 19.08 | 62.07 | 28.83 | 52.04 | 27.37 | 49.4 |
| 1500–3500 | 31.11 | 50.49 | 29.81 | 48.36 | 19.39 | 65.76 | 18.51 | 62.76 | 28.2 | 52.44 | 26.77 | 49.79 |
| 3500–8000 | 30.34 | 51.29 | 29.06 | 49.13 | 18.6 | 66.8 | 17.75 | 63.75 | 27.44 | 53.17 | 26.05 | 50.48 |
| 8000–13000 | 29.21 | 52.02 | 27.98 | 49.83 | 17.74 | 67.42 | 16.93 | 64.34 | 26.35 | 53.79 | 25.02 | 51.07 |
| 13000–15000 | 28.37 | 53.25 | 27.17 | 51.01 | 16.92 | 68.55 | 16.14 | 65.41 | 25.51 | 55.06 | 24.22 | 52.27 |

**Table 4**
The design parameters and performance indexes of the selected points for optimization procedure II.

| Parameter | Unit | Point A | Point B | Point C |
|---|---|---|---|---|
| S/C | - | 4.90 | 3.52 | 4.89 |
| Current density | $A.m^{-2}$ | 1017 | 3998 | 1938 |
| $T_B$ | K | 1229.1 | 1152.1 | 1228.1 |
| Aux/Proc fuel ratio | - | 0.138 | 0.134 | 0.128 |
| Total heat recovered by micro-CHP system | MWh | 740.38 | 957.7 | 760.31 |
| Total electricity provided by micro-CHP system | MWh | 430.41 | 262.8 | 385.58 |
| Total natural gas consumed by the micro-CHP system | $m^3$ | 146880 | 146360 | 145590 |
| Average net electricity output by the micro-CHP system | kW | 28.69 | 17.52 | 25.70 |
| Average heat recovered by the micro-CHP system | kW | 49.36 | 63.85 | 50.69 |
| Cumulative net electrical efficiency of the micro-CHP system | % | 29.96 | 18.36 | 27.07 |
| Cumulative thermal efficiency of the micro-CHP system | % | 51.53 | 66.90 | 53.39 |
| Capital cost | € | 115711 | 39929 | 68398 |
| Income of produced electricity | € | 73170 | 44679 | 65549 |
| Income of produced heat | € | 39247 | 50766 | 40303 |
| Lifecycle cost | € | 85146 | 16736 | 37962 |
| Unit cost of plant | €/kW | 2770 | 2026 | 2461 |

It was demonstrated that an attempt to achieve the highest possible efficiency results in an optimal point with the cumulative electrical efficiency of 29.96% while requiring a capital cost of 115711 €. The optimal point with the lowest required capital cost (39929 €) leads to a cumulative net electrical efficiency of 18.36%. Finally, it was demonstrated that by employing an optimal point in which the same fuel cell area as that of initial design is utilized, a cumulative net electrical efficiency of 27.07% can be obtained which is almost 1% higher than the one which was obtained using the initial design.

## Acknowledgement

This work was carried out in the framework of the project Microgen30 (EE01_00013) funded by Italian Ministry of Economic Development with the program Industra2015. The authors would also like to acknowledge ICI Caldaie S.p.A for providing technical support for this project.

## Nomenclature

*Acronyms*

| | |
|---|---|
| aux/proc | Auxiliary to process flow rate ratio |
| CHP | Combined heat and power |
| GDL | Gas diffusion layer |
| HT-PEM | High temperature proton exchange membrane |
| LCC | Lifecycle cost |
| LT-PEM | Low temperature proton exchange membrane |
| MEA | Membrane electrode assembly |
| OHM | Ohmic |
| PBI | Polybenzimidazole |
| PES | Primary energy saving |
| PFSA | Perfluorosulfonic acid |
| PrOX | Preferential oxidation |
| RF | Reforming factor |
| S/C | Steam to carbon ratio |
| SMR | Steam methane reforming |
| TCC | Total capital cost |
| TER | Thermal to electric ratio |
| WGS | Water gas shift |
| WKO | Water knock out |

*Symbols*

| | |
|---|---|
| $E_{ID}$ | Ideal voltage (V) |
| $\dot{m}$ | Mass flow rate (kg $s^{-1}$) |
| $\Delta H_{298K}$ | Standard enthalpy of reaction (kJ $kmol^{-1}$) |
| $\dot{Q}$ | The time rate of heat transfer (kW) |
| R | Universal gas constant (kJ $kmol^{-1} K^{-1}$) |
| $E_a$ | Activation energy (kJ $mol^{-1}$) |
| F | Friction factor |
| I | Current (A) |
| K | Equilibrium constant |
| K | Rate coefficient |
| LHV | Low heating value (kJ $kg^{-1}$) |
| N | Number of cells |
| Nu | Nusselt number |
| P | Power (kW) |
| Pr | Prandtl number |
| $P_x$ | Partial pressure of species x |
| R | Rate of reaction (mol $lit^{-1} s^{-1}$) |
| Re | Reynolds number |
| T | Temperature (K) |
| V | Voltage (V) |

*Subscripts*

| | |
|---|---|
| A | Anode |
| B | Burner |
| C | Cathode |
| cogen | Cogeneration |
| el | Electrical |
| th | Thermal |

*Greek symbols*

| | |
|---|---|
| $\eta_A$ | Anodic voltage loss |
| $\eta_C$ | Cathodic voltage loss |
| $\eta_{el}$ | Electrical efficiency |
| $\eta_I$ | First law efficiency |
| $\eta_{th}$ | Thermal efficiency |
| $\lambda_{H_2}$ | Anodic stoichiometric ratio |

## References

[1] A. Bazyari, A.A. Khodadadi, A. Haghighat Mamaghani, J. Beheshtian, L.T. Thompson, Y. Mortazavi, Microporous titania–silica nanocomposite catalyst-adsorbent for ultra-deep oxidative desulfurization, Appl. Catal. B Environ. 180 (2016) 65–77.
[2] A. Haghighat Mamaghani, S. Fatemi, M. Asgari, Investigation of influential parameters in deep oxidative desulfurization of dibenzothiophene with hydrogen peroxide and formic acid, Int. J. Chem. Eng. 2013 (2013) 951045.
[3] B. Shabani, J. Andrews, Hydrogen and fuel cells, Green Energy Technol. 201 (2015) 453–491.
[4] A. Adam, E.S. Fraga, D.J.L. Brett, Options for residential building services design using fuel cell based micro-CHP and the potential for heat integration, Appl. Energy 138 (2015) 685–694.
[5] H.R. Ellamla, I. Staffell, P. Bujlo, B.G. Pollet, S. Pasupathi, Current status of fuel cell based combined heat and power systems for residential sector, J. Power Sources 293 (2015) 312–328.

[6] I. Staffell, R. Green, The cost of domestic fuel cell micro-CHP systems, Int. J. Hydrogen Energy 38 (2013) 1088–1102.
[7] F. Rinaldi, R. Marchesi, Polimeric electrolyte membrane fuel cells: characterization test under variable temperature and relative humidity conditions, J. Fuel Cell Sci. Technol. 4 (2007) 231–237.
[8] A. Ferguson, V. Ismet Ugursal, Fuel cell modelling for building cogeneration applications, J. Power Sources 137 (2004) 30–42.
[9] M. Radulescu, O. Lottin, M. Feidt, C. Lombard, D. Le Noc, S. Le Doze, Experimental and theoretical analysis of the operation of a natural gas cogeneration system using a polymer exchange membrane fuel cell, Chem. Eng. Sci. 61 (2006) 743–752.
[10] C.-E. Hubert, P. Achard, R. Metkemeijer, Study of a small heat and power PEM fuel cell system generator, J. Power Sources 156 (2006) 64–70.
[11] M.Y. El-Sharkh, A. Rahman, M.S. Alam, Evolutionary programming-based methodology for economical output power from PEM fuel cell for micro-grid application, J. Power Sources 139 (2005) 165–169.
[12] N. Zuliani, R. Taccani, Microcogeneration system based on HTPEM fuel cell fueled with natural gas: performance analysis, Appl. Energy 97 (2012) 802–808.
[13] A. Arsalis, M.P. Nielsen, S.K. Kær, Modeling and parametric study of a 1 kWe HT-PEMFC-based residential micro-CHP system, Int. J. Hydrogen Energy 36 (2011) 5010–5020.
[14] E. Jannelli, M. Minutillo, A. Perna, Analyzing microcogeneration systems based on LT-PEMFC and HT-PEMFC by energy balances, Appl. Energy 108 (2013) 82–91.
[15] B. Najafi, A. Haghighat Mamaghani, F. Rinaldi, A. Casalegno, Long-term performance analysis of an HT-PEM fuel cell based micro-CHP system: operational strategies, Appl. Energy 147 (2015) 582–592.
[16] P. Mocotéguy, B. Ludwig, J. Scholta, Y. Nedellec, D.J. Jones, J. Rozière, Long-term testing in dynamic mode of HT-PEMFC H3PO 4/PBI celtec-P based membrane electrode assemblies for micro-CHP applications, Fuel Cells 10 (2010) 299–311.
[17] A. Haghighat Mamaghani, B. Najafi, A. Shirazi, F. Rinaldi, 4E analysis and multi-objective optimization of an integrated MCFC (molten carbonate fuel cell) and ORC (organic Rankine cycle) system, Energy 82 (2015) 650–663.
[18] A.H. Mamaghani, B. Najafi, A. Shirazi, F. Rinaldi, Exergetic, economic, and environmental evaluations and multi-objective optimization of a combined molten carbonate fuel cell-gas turbine system, Appl. Therm. Eng. 77 (2015) 1–11.
[19] R. Soltani, P. Mohammadzadeh Keleshtery, M. Vahdati, M.H. Khoshgoftarmanesh, M.A. Rosen, M. Amidpour, Multi-objective optimization of a solar-hybrid cogeneration cycle: application to CGAM problem, Energy Convers. Manag. 81 (2014) 60–71.
[20] G.L. Guizzi, M. Manno, Fuel cell-based cogeneration system covering data centers' energy needs, Energy 41 (2012) 56–64.
[21] A.D. Hawkes, P. Aguiar, C.A. Hernandez-Aramburo, M.A. Leach, N.P. Brandon, T.C. Green, et al., Techno-economic modelling of a solid oxide fuel cell stack for micro combined heat and power, J. Power Sources 156 (2006) 321–333.
[22] M. Bianchi, A. De Pascale, P.R. Spina, Guidelines for residential micro-CHP systems design, Appl. Energy 97 (2012) 673–685.
[23] J. Xu, G.F. Froment, Methane steam reforming, methanation and water-gas shift: I. Intrinsic kinetics, AIChE J. 35 (1989) 88–96.
[24] R.L. Keiski, T. Salmi, P. Niemistö, J. Ainassaari, V.J. Pohjola, Stationary and transient kinetics of the high temperature water-gas shift reaction, Appl. Catal. A Gen. 137 (1996) 349–370.
[25] A. Posada, V. Manousiouthakis, Heat and power integration of methane reforming based hydrogen production†, Ind. Eng. Chem. Res. 44 (2005) 9113–9119.
[26] C. Siegel, G. Bandlamudi, A. Heinzel, Systematic characterization of a PBI/H3PO4 sol–gel membrane – Modeling and simulation, J. Power Sources 196 (2011) 2735–2749.
[27] L. Pisani, Multi-component gas mixture diffusion through porous media: a 1D analytical solution, Int. J. Heat Mass Transf. 51 (2008) 650–660.
[28] Z. Liu, J.S. Wainright, M.H. Litt, R.F. Savinell, Study of the oxygen reduction reaction (ORR) at Pt interfaced with phosphoric acid doped polybenzimidazole at elevated temperature and low relative humidity, Electrochim. Acta 51 (2006) 3914–3923.
[29] J.J. Baschuk, X. Li, Modelling CO poisoning and O2 bleeding in a PEM fuel cell anode, Int. J. Energy Res. 27 (2003) 1095–1116.
[30] A. Bergmann, D. Gerteisen, T. Kurz, Modelling of CO Poisoning and its dynamics in HTPEM fuel cells, Fuel Cells 10 (2010) 278–287.
[31] B. Najafi, A. Haghighat Mamaghani, A. Baricci, F. Rinaldi, A. Casalegno, Mathematical modelling and parametric study on a 30 kWel high temperature PEM fuel cell based residential micro cogeneration plant, Int. J. Hydrogen Energy 40 (2015) 1569–1583.
[32] M. Wei, T. McKone, A Total Cost of Ownership Model for Design and Manufacturing Optimization of Fuel Cells in Stationary and Emerging Market Applications, Presented by Lawrence Berkeley National Laboratory at Department of Energy Annual Merit Review for Fuel Cell Research, Arlington, VA, 2013.
[33] A. Arsalis, Modeling and simulation of a 100 kWe HT-PEMFC subsystem integrated with an absorption chiller subsystem, Int. J. Hydrogen Energy 37 (2012) 13484–13490.
[34] A. Shirazi, B. Najafi, M. Aminyavari, F. Rinaldi, R.A. Taylor, Thermal–economic–environmental analysis and multi-objective optimization of an ice thermal energy storage system for gas turbine cycle inlet air cooling, Energy 69 (2014) 212–226.
[35] M. Aminyavari, B. Najafi, A. Shirazi, F. Rinaldi, Exergetic, economic and environmental (3E) analyses, and multi-objective optimization of a CO 2/NH 3 cascade refrigeration system, Appl. Therm. Eng. 65 (2014) 42–50.
[36] B. Najafi, A.H. Mamaghani, F. Rinaldi, A. Casalegno, Fuel partialization and power/heat shifting strategies applied to a 30 kW el high temperature PEM fuel cell based residential micro cogeneration plant, Int. J. Hydrogen Energy 40 (2015) 14224–14234.
[37] J. Kim, M. Kim, T. Kang, Y.-J. Sohn, T. Song, K.H. Choi, Degradation modeling and operational optimization for improving the lifetime of high-temperature PEM (proton exchange membrane) fuel cells, Energy 66 (2014) 41–49.